

---

# Performance of Advanced Automotive Fuel Cell Stacks and Systems with State-of-the-Art d-PtCo/C Cathode Catalyst in Membrane Electrode Assemblies

Rajesh K. Ahluwalia (Primary Contact),  
Xiaohua Wang, and J-K Peng  
Argonne National Laboratory  
9700 South Cass Avenue  
Lemont, IL 60439  
Phone: (630) 252-5979; Fax: (630) 252-5161  
Email: [walia@anl.gov](mailto:walia@anl.gov)

DOE Manager: Nancy L. Garland  
Phone: (202) 586-5673  
Email: [Nancy.Garland@ee.doe.gov](mailto:Nancy.Garland@ee.doe.gov)

Project Start Date: October 1, 2003  
Project End Date: Project continuation and  
direction determined annually by DOE

- Provide modeling support to Strategic Analysis, Inc. in annual update of progress in meeting technical targets, including FCS cost.

## Technical Barriers

This project addresses the following technical barriers from the Fuel Cells section of the Fuel Cell Technologies Office Multi-Year Research, Development, and Demonstration Plan<sup>1</sup>:

- (A) Durability
- (B) Cost
- (C) Performance.

## Technical Targets

This project focuses on conducting system-level analyses to address the following DOE 2020 technical targets for automotive fuel cell power systems operating on direct hydrogen:

- Energy efficiency: 60% at 25% of rated power
- $Q/\Delta T$ : 1.45 kW/°C
- Power density: 850 W/L for system, 2,500 W/L for stack
- Specific power: 850 W/kg for system, 2,000 W/kg for stack
- Transient response: 1 second from 10% to 90% of maximum flow
- Start-up time: 30 seconds from -20°C and 5 seconds from +20°C ambient temperature
- Precious-metal content: 0.125 g/kW<sub>e</sub> rated gross power.

## Overall Objectives

- Develop a validated model for automotive fuel cell systems, and use it to assess the status of the technology.
- Conduct studies to improve performance and packaging, to reduce cost, and to identify key R&D issues.
- Compare and assess alternative configurations and systems for transportation and stationary applications.
- Support DOE/U.S. DRIVE automotive fuel cell development efforts.

## Fiscal Year (FY) 2018 Objectives

- Modify the reference fuel cell system (FCS) configuration to include controls for extended stack durability on operational, start-up, and shut-down transients.
- Quantify the impact of low-platinum group metal (PGM) alloy catalysts on the performance of automotive stacks and fuel cell systems.

---

<sup>1</sup> <https://www.energy.gov/eere/fuelcells/downloads/fuel-cell-technologies-office-multi-year-research-development-and-22>

## FY 2018 Accomplishments

- Projected  $46.0 \pm 0.7$   $\$/kW_e$  FCS cost at 500,000 units per year, and  $8.5 \pm 0.4$   $kW_e/g$  FCS Pt utilization with state-of-the-art (SOA) d-PtCo/C cathode catalyst, reinforced 14- $\mu m$  850 equivalent weight membrane, and  $Q/\Delta T = 1.45$   $kW/^\circ C$  constraint.
- Verified that the SOA catalyst system can achieve  $1,180 \pm 55$   $mW/cm^2$  stack power density, exceeding the target  $1,000$   $mW/cm^2$  at low Pt loading ( $0.125$   $mg-Pt/cm^2$  total).
- Projected  $<5\%$  penalty in power density if the cathode humidifier is removed, and  $\sim 15\%$  penalty if stack inlet pressure is reduced to 2 atm from 2.5 atm.
- Showed that parasitic power approaches  $25$   $kW_e$  if the compressor discharge pressure is raised to 4 atm.
- Modified the reference system configuration to include valves and controls for protected shutdown, safe startup from sub-freezing temperatures, and limiting cell voltage to  $0.85$ – $0.875$  V during idle.

## INTRODUCTION

While different developers are addressing improvements in individual components and subsystems in automotive fuel cell propulsion systems (i.e., cells, stacks, balance-of-plant components), we are using modeling and analysis to address issues of thermal and water management, design-point and part-load operation, and component-, system-, and vehicle-level efficiencies and fuel economies. Such analyses are essential for effective system integration.

## APPROACH

Two sets of models are being developed. The GCtool software is a standalone code with capabilities for design, off-design, steady-state, transient, and constrained optimization analyses of fuel cell systems. A companion code, GCtool-ENG, has an alternative set of models with a built-in procedure for translation to the MATLAB/SIMULINK platform commonly used in vehicle simulation codes, such as Autonomie.

## RESULTS

For extended durability, we modified the reference system to incorporate valves (see Figure 1) and controls for protected shutdown, safe startup from below-freezing temperatures, and limiting cell voltage at idle. We developed a model to show that the cell voltage can be maintained below 0.85 V during idle by reducing the cathode stoichiometry to 1.05, or by increasing the stack temperature to more than 80°C, while limiting the minimum stack power to 2.8–3.0 kW<sub>e</sub>. We analyzed the possibility of further decreasing the idle cell voltage with wider latitude in minimum power by decreasing O<sub>2</sub> concentration at stack inlet by recycling cathode spent air and bypassing the stack. We also developed a protected shutdown algorithm that involves closing the stack bypass and isolation valves to deplete O<sub>2</sub> in the cathode channels during shutdown, ensuring that damaging H<sub>2</sub>-air fronts cannot form in the anode channels during subsequent start-up. Following our earlier work [1], we are analyzing a method of preventing icing by maximizing in-stack heat production during sub-freeze start by operating at low cell voltages.

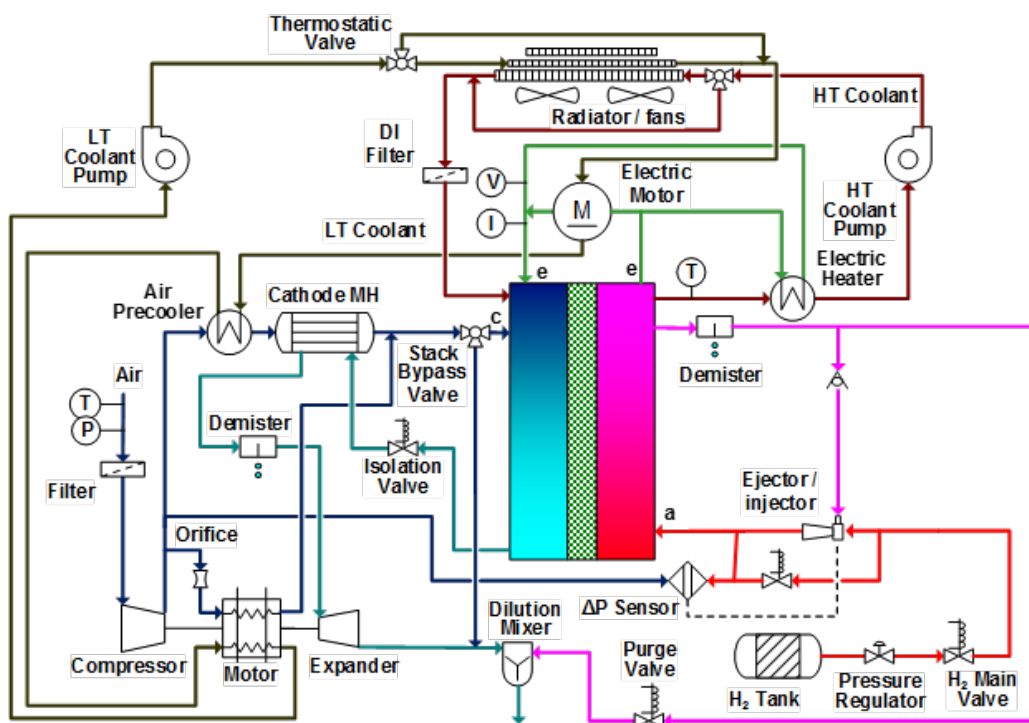


Figure 1. Argonne 2018 FCS configuration with controls

We evaluated the performance of a SOA d-PtCo catalyst supported on high-surface-area carbon in cathode and Pt catalyst supported on Vulcan carbon in anode. The Pt loadings are 0.1 mg/cm<sup>2</sup> in the cathode catalyst and 0.025 mg/cm<sup>2</sup> in the anode catalyst. Figure 2a lists other attributes of the membrane electrode assembly (MEA) containing these catalysts. We collaborated with the Fuel Cell Consortium for Performance and Durability (FC-PAD) funding opportunity announcement project led by General Motors in testing cells with this MEA on a United States–European Union (U.S.-EU) differential cell hardware shown in Figure 2b. The tests were run using two different protocols, random and controlled. The random protocol used semi-statistical ordering of a test matrix with multiple variables, forward scans, and a 3-minute hold at each cell voltage. The controlled protocol used model-guided single-variable tests with some two-variable tests, forward scans, and 3-minute hold at each cell voltage. As in earlier work [2], we determined the kinetic performance of d-PtCo/C catalyst by using the measured polarization data at low-current densities together with the ionic conductivity ( $\sigma_c$ ) of the cathode catalyst layer (CCL) derived from the galvanostatic impedance data obtained in H<sub>2</sub>/N<sub>2</sub>, and a transient solid solution model for oxide coverage ( $\theta$ ) as a function of potential, relative humidity ( $\Phi$ ), and temperature ( $T$ ). Figure 2c lists the derived kinetic constants appearing in the following distributed kinetic model for the oxygen reduction reaction (ORR).

$$\eta_c = \eta_s^c + iR_{\Omega}^c \left( \frac{i\delta_c}{b\sigma_c} \right)$$

$$i + i_x = i_0 S_{Pt} (1 - \theta) e^{-\frac{\omega\theta}{RT}} e^{\frac{\alpha n F}{RT} \eta_s^c}$$

$$i_0 = i_{0r} e^{-\frac{\Delta H_s^c}{R} \left( \frac{1}{T} - \frac{1}{T_r} \right)} P_{O_2}^{\gamma} \Phi^{\beta}$$

Figure 2d compares the mass activity of the cathode catalyst calculated using the kinetic model with the data for other catalyst systems investigated in this project. Some main conclusions from this comparison are highlighted below.

- d-PtCo/C has 2 times the modeled mass activity of the annealed Pt catalyst (a-Pt/C) that has nearly the same particle size.
- d-PtCo/C and d-PtNi/C alloy have comparable mass activities.
- Both low-PGM alloy catalysts (d-PtNi/C and d-PtCo/C) meet the mass activity targets of 440 A/g<sub>Pt</sub>.

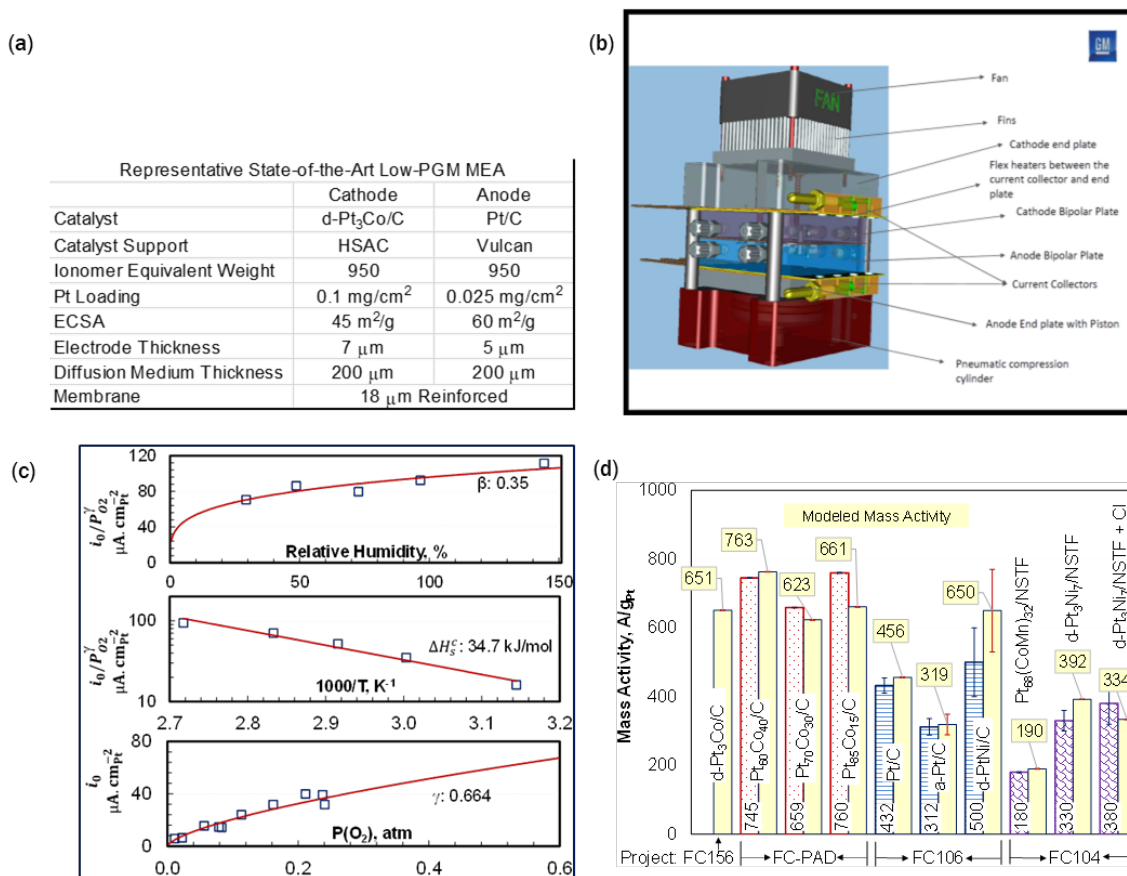


Figure 2. ORR kinetics model: (a) representative state-of-the-art low-PGM MEA; (b) U.S.-EU differential cell hardware; (c) modeled kinetics of ORR on SOA d-PtCo/C catalyst; and (d) comparison of mass activity with other dispersed Pt and Pt alloy catalysts and binary and ternary nanostructured thin film catalysts. Solid fills are modeled values from ORR kinetic model; pattern fills are measured mass activities in H<sub>2</sub>/O<sub>2</sub>.

We characterized the high-current-density performance of the MEA by developing a correlation for mass transfer overpotential ( $\eta_m$ ) in terms of the limiting current density ( $i_L$ ) at which  $\eta_m$  equals 400 mV. The limiting current density was modeled as a function of pressure, CCL temperature ( $T_c$ ), CCL relative humidity ( $\Phi_c$ ) and O<sub>2</sub> partial pressure ( $P_{O_2}$ ) in gas channel (see Figure 3a). We formulated heat and mass transfer models to determine  $T_c$  and  $\Phi_c$  as functions of bipolar plate temperature, Nernst potential, cell voltage, current density, and water transport across membrane. Some conclusions from the results in Figure 3 are noted below.

- For given pressure (P),  $i_L$  in Figure 3b increases with increase in  $P(O_2)$ . However, for given  $P(O_2)$ ,  $i_L$  in Figure 3b and 3c is smaller at greater pressures because of the inverse dependence of O<sub>2</sub> gas phase diffusivity on pressure. The decrease in  $i_L$  is less than proportional to 1/P, implying that non-Fickian diffusion controls mass transport resistance.
- At constant  $X(O_2)$ ,  $i_L$  in Figure 3d increases with increase in pressure because of higher  $P(O_2)$ . The increase in  $i_L$  is somewhat less than proportional to  $P(O_2)$ , implying that mass transport resistance also increases with  $P(O_2)$ .
- Dependence of  $i_L$  on  $T_c$  in Figure 3e is greater than  $T^{3/2}$ , confirming that processes other than Fickian diffusion are rate controlling, particularly O<sub>2</sub> permeability through the ionomer film on the catalyst particles.

- For given  $T_c$ ,  $i_L$  in Figure 3f is highest at an intermediate relative humidity in CCL ( $\phi_c^*$ ) indicating that CCL floods for  $\phi_c > \phi_c^*$ . Figure 3f shows that  $\phi_c^*$  increases at higher  $T_c$ .

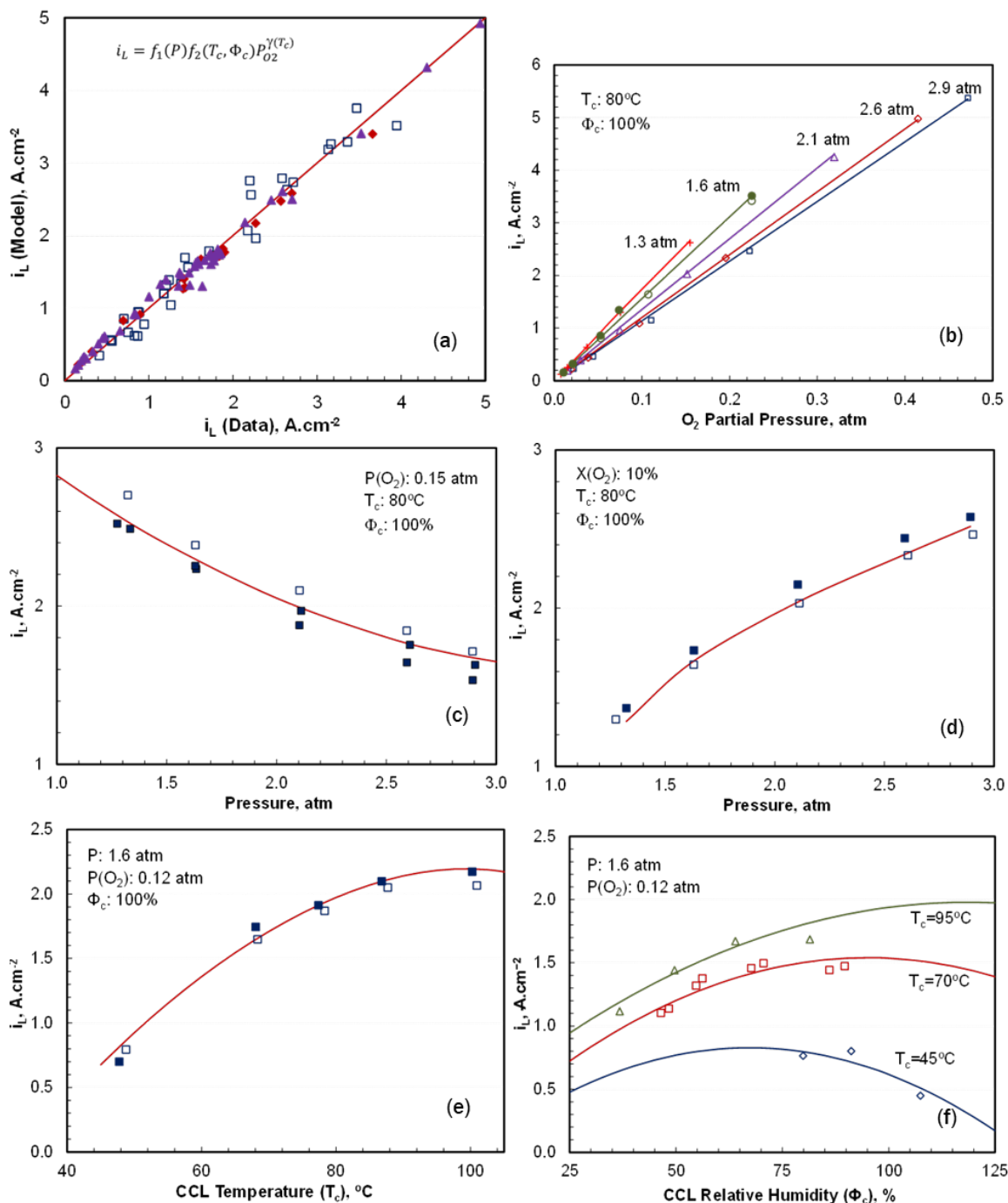


Figure 3. Oxygen mass transfer and limiting current density: (a) limiting current density model calibration; (b) effect of operating pressure and oxygen partial pressure; (c) effect of operating pressure for fixed  $P(O_2)$ ; (d) effect of operating pressure for fixed  $X(O_2)$ ; (e) effect of CCL temperature; and (f) effect of CCL relative humidity

Following the methodology formulated previously [2, 3], we developed an integral cell model using the differential cell data in Figure 2 and Figure 3 to evaluate the performance and cost of an automotive fuel cell system with the SOA d-PtCo/C catalyst relative to 2020 targets of 65% peak efficiency,  $Q/\Delta T$  of 1.45 kW/K,

and \$40/kW cost. The Pt loadings are 0.1 mg/cm<sup>2</sup> in the cathode catalyst and 0.025 mg/cm<sup>2</sup> in the anode catalyst. The 850-EW PFSA membrane is 14 μm thick, chemically stabilized, and mechanically reinforced. All other main attributes of the system components and operating conditions are summarized in Table 1.

**Table 1. Rated Power Performance of FCS with SOA Alloy Catalysts**

Stack Parameters	2018 FCS with d-PtCo/C Catalyst	2017 FCS with d-PtNi/C Catalyst
Membrane	Ionomer: 850 EW PFSA with chemical additive Substrate: Mechanical reinforcement Thickness: 14 μm	Ionomer: 850 EW PFSA with chemical additive Substrate: Mechanical reinforcement Thickness: 14 μm
Cathode Catalyst	d-Pt <sub>3</sub> Co/C (0.1 mg <sub>Pt</sub> /cm <sup>2</sup> ), EW=950, I/C=1.0	Electrode: d-PtNi <sub>3</sub> (0.1 mg <sub>Pt</sub> /cm <sup>2</sup> ), acid washed Ink: organic, EW=850, I/C=1.0
Anode Catalyst	Pt/C (0.025 mg <sub>Pt</sub> /cm <sup>2</sup> )	Pt/C (0.025 mg <sub>Pt</sub> /cm <sup>2</sup> )
Stack Gross Power	88.5 kW	88.1 kW
Stack Voltage (Rated)	250 V	250 V
Number of Active Cells	380 cells (also 381 cooling cells)	377 cells (also 376 cooling cells)
Stack Gross Power Density	3.07 kW/L	2.84 kW/L
Stack Gross Specific Power	3.73 kW/kg	3.45 kW/kg
Stack Inlet Pressure	2.5 bar	2.5 bar
Stack Coolant Temperature	85°C (inlet), 95°C (outlet)	84°C (inlet), 94°C (outlet)
Stack Air Inlet/Outlet RH	Inlet: 51% RH at 85°C; Outlet: 77% RH at 95°C	Inlet: 75% RH at 84°C; Outlet: 100% RH at 94°C
Stack Fuel Inlet/Outlet RH	Inlet: 42% RH at 95°C; Outlet: 160% RH at 85°C	Inlet: 42% RH at 94°C; Outlet: 100% RH at 84°C
Cathode/Anode Stoichiometry	1.5 (cathode) / 2.0 (anode)	1.5 (cathode) / 2.0 (anode)
Cell Area	197 cm <sup>2</sup> (active), 320 cm <sup>2</sup> (total)	213 cm <sup>2</sup> (active), 346 cm <sup>2</sup> (total)
Cell Voltage	657.1 mV	663 mV
Current Density	1.8 A/cm <sup>2</sup>	1.651 A/cm <sup>2</sup>
Crossover Current Density	4.2 mA/cm <sup>2</sup> @ 80°C, 100% RH, 1 atm P <sub>H<sub>2</sub></sub>	4.2 mA/cm <sup>2</sup> @ 80°C, 100% RH, 1 atm P <sub>H<sub>2</sub></sub>
Power Density	1183 mW/cm <sup>2</sup>	1095 mW/cm <sup>2</sup>
<b>Balance of Plant</b>		
Humidifier Membrane Area	0.68 m <sup>2</sup>	0.8 m <sup>2</sup>
Air Pre-cooler Heat Duty	6.3 kW	6.3 kW
CEM Motor and Motor Controller Heat Duty	3.1 kW	3.0 kW
Main Radiator Heat Duty	87.3 kW	78.9 kW
CEM Power	Compressor shaft power: 10.4 kW Expander shaft power out: 4.5 kW Net motor and motor controller: 7.4 kW <sub>e</sub>	Compressor shaft power: 10.3 kW Expander shaft power out: 4.7 kW Net motor and motor controller: 7.0 kW <sub>e</sub>
Fan and Pump Parasitic Power	0.6 kW <sub>e</sub> (coolant pump), 0.3 kW <sub>e</sub> (H <sub>2</sub> recirculation pump), 0.345 kW <sub>e</sub> (radiator fan)	0.5 kW <sub>e</sub> (coolant pump), 0.3 kW <sub>e</sub> (H <sub>2</sub> recirculation pump), 0.345 kW <sub>e</sub> (radiator fan)

Figure 4a presents the cost of the fuel cell system at different stack inlet pressures and stack coolant outlet temperatures. The results in Figure 4a confirm the FY 2017 landmark conclusion that at high manufacturing volume (500,000 units/year), the projected system cost can be 46.0 ± 0.7 \$/kW<sub>e</sub> at 2.5 atm stack inlet pressure and 95°C stack coolant outlet temperature. Removing the membrane humidifier slightly reduces the system cost at 2.5 atm stack inlet pressure. These results are based on Strategic Analysis, Inc.’s 2018 cost correlation that includes a \$2.01/kW<sub>e</sub> increase for manufacturing bipolar plates and MEAs, added controls for extended durability, and compressor-expander-motor module price inflation [4].

Pending model validation against data from a 50-cm<sup>2</sup> integral cell, the results in Figure 4a should be regarded as preliminary. The error bars reflect variance of kinetic data in random and controlled tests and include degradation between the two series of tests. We also estimated the system cost at lower manufacturing volumes as 51 \$/kW<sub>e</sub> at 100,000 units/year, and 88 \$/kW<sub>e</sub> at 10,000 units/year.

In Figure 4, (b) and (c) present the modeled stack and FCS platinum utilization and confirm the FY 2017 results that the stack Pt utilization (9.5 ± 0.5 kW<sub>e</sub>/g) with the SOA catalyst exceeds the DOE target (8.0 kW<sub>e</sub>/g). Even on a system basis, the modeled FCS Pt utilization (8.5 ± 0.4 kW<sub>e</sub>/g) exceeds the stack target. The results indicate that stack inlet pressures greater than 2.0 atm are needed to meet the Pt utilization target.

Figure 4d presents the modeled stack power density and confirms the FY 2017 result that with the SOA catalyst the gross stack power density ( $1,180 \pm 55 \text{ mW/cm}^2$ ) greatly exceeds the target ( $1,000 \text{ mW/cm}^2$ ) at low Pt loading ( $0.125 \text{ mg-Pt/cm}^2$  total). Also, stack inlet pressures greater than 2.0 atm are needed to meet the power density target.

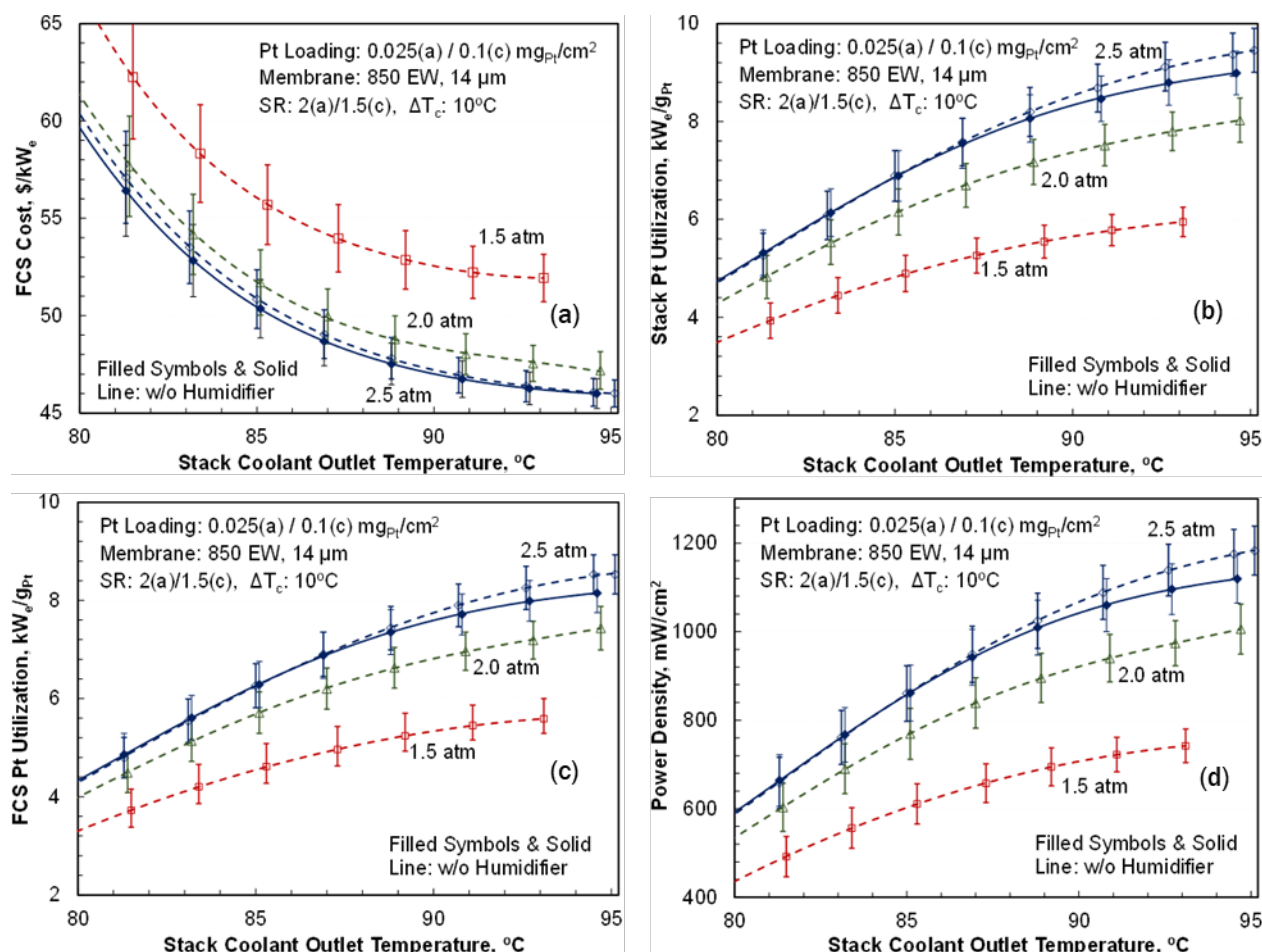


Figure 4. FCS performance with SOA d-PtCo/C cathode electrode: (a) FCS cost at high-volume manufacturing (50,000 units/year); (b) stack Pt utilization; (c) FCS Pt utilization; (d) stack power density

### CONCLUSIONS AND UPCOMING ACTIVITIES

- We have shown that minimal controls are needed to extend stack durability by maintaining the cell voltage below 0.85 V during idle and to implement protected shutdown strategies by depleting O<sub>2</sub> in the cathode channels during shutdown, ensuring that damaging H<sub>2</sub>-air fronts cannot form in the anode channels during subsequent start-up.
- We demonstrated that SOA d-Pt<sub>3</sub>Co/high-surface-area carbon cathode catalysts in MEAs can lead to power densities exceeding the 2020 target of  $1,000 \text{ mW/cm}^2$  at  $0.125 \text{ g/kW}_e$  PGM content under operating conditions ( $95^\circ\text{C}$ ,  $<100\%$  outlet relative humidity, SR(c) = 1.5, 2.5 atm stack inlet pressure) required to meet the heat rejection constraint ( $Q/\Delta T = 1.45 \text{ kW/}^\circ\text{C}$ ). We also showed that stack Pt utilization exceeding the target of  $8.0 \text{ kW}_e/\text{g}_{\text{Pt}}$  can be achieved with this catalyst system.
- We confirmed the FY 2017 landmark conclusion that at high manufacturing volume (500,000 units/year), the projected system cost can be  $46.0 \pm 0.7 \text{ } \$/\text{kW}_e$  at 2.5 atm stack inlet pressure and  $95^\circ\text{C}$  stack coolant outlet temperature. This projection is based on Strategic Analysis, Inc.’s 2018 cost



correlation that includes \$2.01/kW<sub>e</sub> increase for manufacturing bipolar plates and MEAs, added controls for extended durability, and compressor-expander-motor module price inflation. At reduced manufacturing volumes, the projected costs increase to \$51/kW<sub>e</sub> at 100,000 units per year and \$88/kW<sub>e</sub> at 10,000 units per year.

- Our future work will focus on durability of low-loaded d-PtCo/C catalysts under cyclic potentials and on automotive drive cycles.

## FY 2018 PUBLICATIONS/PRESENTATIONS

1. R.K. Ahluwalia, “Performance and Durability of Advanced Automotive Fuel Cell Stacks and Systems with Dispersed Alloy Cathode Catalyst in Membrane Electrode Assemblies,” 2017 Technology Collaboration Program on Advanced Fuel Cells—Topical Meeting on Catalysis, Berlin, Germany, November 14, 2017.
2. R.K. Ahluwalia and N. Garland, “Reports from the Annexes: Annex 34: Fuel Cells for Transportation,” 55th ExCo Meeting, Berlin, Germany, November 14–17, 2017.
3. R.K. Ahluwalia, D.D. Papadimas, N.N. Kariuki, J.-K. Peng, X. Wang, Y. Tsai, D.G. Graczyk, and D.J. Myers, “Potential Dependence of Pt and Co Dissolution from Platinum-Cobalt Alloy PEFC Catalysts Using Time-Resolved Measurements,” *Journal of the Electrochemical Society* 165, no. 6 (2018): F3024–F3035.
4. R.K. Ahluwalia, F.C. Cetinbas, J.-K. Peng, N.N. Kariuki, and D.J. Myers “Reconstruction and Modeling of Electrode Microstructure Using Nano X-ray Computed Tomography,” 2017 Fuel Cell Consortium for Performance and Durability Meeting, Southfield, Michigan, July 19, 2017.
5. R.K. Ahluwalia, X. Wang, and D.D. Papadimas, “Performance and Stability of Bipolar Plates for Automotive Fuel Cells,” Shanghai Jiaotong University, Shanghai, China, September 26, 2017.
6. R.K. Ahluwalia, X. Wang, and J.-K. Peng, “Performance and Durability of Advanced Automotive Fuel Cell Stacks and Systems with Dispersed Alloy Cathode Catalyst in Membrane Electrode Assemblies,” FY 2017 Annual Progress Report, DOE Hydrogen and Fuel Cells Program, DOE/GO-102017-5042, February 2018.
7. R.K. Ahluwalia, X. Wang, and J.-K. Peng, “Performance and Durability of Advanced Automotive Fuel Cell Stacks and Systems with Dispersed Alloy Cathode Catalyst in Membrane Electrode Assemblies,” Topical Meeting on Catalysis, IEA Energy Technology Network, Technology Collaboration Program on Advanced Fuel Cells, Berlin, Germany, November 15, 2017.
8. R.K. Ahluwalia, X. Wang, J.-K. Peng, and D.D. Papadimas, “Fuel Cell System Modeling and Analysis,” US Drive Fuel Cell Tech Team Meeting, Southfield, Michigan, February 21, 2018.
9. R.K. Ahluwalia, X. Wang, J.-K. Peng, N.N. Kariuki, D.J. Myers, S. Rasouli, P.J. Ferreira, Z. Yang, A. Martinez-Bonastre, D. Fongalland, and J. Sharman, “Durability of De-Alloyed Platinum-Nickel Cathode Catalyst in Low Platinum Loading Membrane-Electrode Assemblies Subjected to Accelerated Stress Tests,” *Journal of the Electrochemical Society* 165, no. 6 (2018): F3316–F3327.
10. R.L. Borup, R. Mukundan, S. Stariha, D.A. Langlois, R. Ahluwalia, D.D. Papadimas, B. Sneed, K.L. More, and S.S. Kocha, “Cathode Carbon Corrosion and Electrode Layer Compaction in PEM Fuel Cells,” 232nd Electrochemical Society Meeting, National Harbor, Maryland, October 1–6, 2017.
11. F.C. Cetinbas, N.N. Kariuki, R.K. Ahluwalia, H.T. Chung, P. Zelanay, and D.J. Myers, “PGM-Free Electrode Microstructure Analysis and Transport Modeling,” 232nd Electrochemical Society Meeting, National Harbor, Maryland, October 1–6, 2017.
12. F.C. Cetinbas, X. Wang, R.K. Ahluwalia, N.N. Kariuki, R.P. Winarski, Z. Yang, J. Sharman, and D.J. Myers, “Microstructural Analysis and Transport Resistances of Low-Platinum-Loaded PEFC Electrodes,” *Journal of the Electrochemical Society* 164, no. 14 (2017): F1596–F1607.

13. N. Kariuki, D.D. Papadias, D.J. Myers, and R.K. Ahluwalia, "Insights into Platinum-Cobalt Electrochemical Dissolution from Platinum-Cobalt Alloy Polymer Electrolyte Fuel Cell Fuel Cell Cathode Catalysts Using Online ICP-MS," 232nd Electrochemical Society Meeting, National Harbor, Maryland, October 1–6, 2017.
14. L. Osmieri, X. Wang, F. Cetinbas, H.T. Chung, X. Yin, S. Kabir, D.J. Myers, P. Zelenay, R. Ahluwalia, and K.C. Neyerlin, "Operando Determination of Oxygen Reduction Reaction Kinetics on PGM-Free Electrocatalysts in a PEFC," 233rd Electrochemical Society Meeting, Seattle, Washington, May 13–17, 2018.
15. D.D. Papadias, R.K. Ahluwalia, N.N. Kariuki, D.J. Myers, K.L. More, D.A. Cullen, B. Sneed, R. Mukundan, R.L. Borup, K.C. Neyerlin, and S.S. Kocha, "Durability of Pt-Co Alloy Cathode Catalysts for PEM Fuel Cells Under Cyclic Potentials," 232nd Electrochemical Society Meeting, National Harbor, Maryland, October 1–6, 2017.
16. D.D. Papadias, R.K. Ahluwalia, N.N. Kariuki, D.J. Myers, K.L. More, D.A. Cullen, B.T. Sneed, K.C. Neyerlin, R. Mukundan, and R.L. Borup, "Durability of Pt-Co Alloy Polymer Electrolyte Fuel Cell Cathode Catalysts Under Accelerated Stress Tests," *Journal of the Electrochemical Society* 165, no. 6 (2018): F3166–F3177.
17. X. Wang, J.-K. Peng, and R.K. Ahluwalia, "Using Differential Cell Data to Predict the Performance of Integral Automotive Fuel Cells," Shanghai Jiaotong University, Shanghai, China, September 26, 2017.
18. X. Wang, R.K. Ahluwalia, J.-K. Peng, F.C. Cetinbas, and D.D. Papadias, "Performance and Durability of Automotive Fuel Cell Stack and System," Research & Advanced Technology, SAIC Motor Corporation Limited, Shanghai, China, September 25, 2017.
19. L. Xin, F. Yang, J. Xie, Z. Yang, N. N. Kariuki, D. J. Myers, J.-K. Peng, X. Wang, R.K. Ahluwalia, K. Yu, P.J. Ferreira, A.M. Bonastre, D. Fongalland, and J. Sharman, "Enhanced MEA Performance for PEMFCs under Low Relative Humidity and Low Oxygen Content Conditions via Catalyst Functionalization," *Journal of the Electrochemical Society* 164, no. 6 (2017): F674–F684.

## REFERENCES

1. R.K. Ahluwalia, and X. Wang, "Rapid Self-Start of Polymer Electrolyte Fuel Cell Stacks from Subfreezing Temperatures," *J. Power Sources* 162 (2006): 502–512.
2. R.K. Ahluwalia, X. Wang, and J.-K. Peng, "Fuel Cell System Modeling and Analysis," DOE Hydrogen and Fuel Cells Program, 2017 Annual Merit Review and Evaluation Meeting, FC017, Washington, D.C., June 5–9, 2017.
3. R.K. Ahluwalia, X. Wang, and A.J. Steinbach, "Performance of Advanced Automotive Fuel Cell Systems with Heat Rejection Constraint," *J. Power Sources* 309 (2016): 178–191.
4. B.D. James, J.M. Huya-Kouadio, and C. Houchins, "Fuel Cell Systems Analysis," 2018 DOE Hydrogen and Fuel Cells Program Review, FC163, Washington, D.C., June 15, 2018.